

An experimental study of kaolinite and dickite relative stability at 150–300 °C and the thermodynamic properties of dickite

ALEXANDRE ZOTOV,^{1,2} ALEXANDRE MUKHAMET-GALEEV,¹ AND JACQUES SCHOTT^{2,*}

¹Institute of Geology of Ore Deposits, Petrography, Mineralogy and Geochemistry, 109017 Moscow, Russia

²Laboratoire de Géochimie, CNRS-OMP-Université Paul-Sabatier, 31400 Toulouse, France

ABSTRACT

The Gibbs free energy ($\Delta G_{(1)}^0$) of the reaction kaolinite \leftrightarrow dickite was generated from solubility measurements of natural kaolinite and dickite performed in acid solutions at temperatures ranging from 150 to 300 °C under vapor-saturated conditions. The $\Delta G_{(1)}^0$ values increase from -0.620 ± 0.150 to -0.218 ± 0.210 kcal/mol with increasing temperature from 150 to 300 °C. Regression of these data yields a value of -0.90 ± 0.10 kcal/mol for $\Delta G_{(1)}^0$ at 25 °C. The standard Gibbs free energy of formation ($\Delta G_{f,298}^0$) of dickite deduced from $\Delta G_{(1)}^0$ and the $\Delta G_{f,298}^0$ of kaolinite (Zotov et al., in preparation) is -908.36 ± 0.40 kcal/mol. The results obtained in this study indicate that kaolinite is metastable relative to dickite at temperatures to at least 350 °C. It follows that the timing of observed kaolinite to dickite transformations in diagenetic and many hydrothermal systems is controlled by the kinetics of this reaction rather than thermodynamic equilibria.

INTRODUCTION

Kaolinite and dickite are the two most widespread polytypes (1Tc and 2M₁, respectively) of the kaolin group of clay minerals (Bailey 1980). Kaolinite generally forms at low temperature (<150 °C) during weathering and diagenetic processes in soils and sedimentary rocks or during epithermal processes. By contrast, dickite occurs in hydrothermally altered rocks formed at higher temperature (150–250 °C) and in sedimentary rocks altered under medium- to high-grade diagenetic conditions. Transformation of kaolinite to dickite is observed in sedimentary basins with increasing burial depth reflecting increasing temperature and pressure (Dunoyer de Segonzac 1970; Shutov et al. 1970; Ehrenberg et al. 1993). Consequently, several authors have suggested that the relative occurrence of these minerals can be used for paleothermometric reconstructions (Kossovskaya and Shutov 1963; Anovitz et al. 1991; Ehrenberg et al. 1993). Based both on the transformation of kaolinite to dickite with increasing depth of burial and on available data on the Gibbs free energy of these minerals at 25 °C (Naumov et al. 1974; Robie et al. 1979; Haas et al. 1981; Robinson et al. 1982), it is generally believed that kaolinite is more stable than dickite at ambient temperature, whereas dickite is more stable at temperatures higher than 150–200 °C. However, available entropy and heat capacity data for these minerals (King and Weller 1961) imply that the ΔS^0 of the reaction kaolinite \leftrightarrow dickite is negative, which is consistent with the fact that the double-layer structure of dickite is more ordered than the one-layer structure of kaolinite. Hence, unlike geological observations, available ther-

modynamic data suggest that dickite is unstable relative to kaolinite at all temperatures.

The present study was initiated to resolve the conflict between available thermodynamic data and geological observations. Toward this goal, kaolinite and dickite solubility were measured at pH from ~ 1 to 2.5 and temperatures from 150 to 300 °C. Taking account of these results, thermodynamic parameters for the kaolinite \leftrightarrow dickite reaction were generated over the temperature range 25–300 °C. These parameters were used to generate an internally consistent set of thermodynamic data for dickite and kaolinite. These results should lead to an improved description of phase relations among aluminosilicate minerals in sedimentary basins and hydrothermal systems.

MATERIALS AND METHODS

Kaolinite and dickite

Pure highly crystalline hydrothermal kaolinite and dickite were used in this study. The two kaolinites investigated are from Glukhovetskoe (Ukraine) and Decazeville (France); these samples have been described in detail by Zotov et al. (in preparation) and Devidal et al. (1996), respectively. Both are well crystallized (Hinkley indices are equal to 1.30 and 1.39, respectively) and contain less than 1 wt% impurities. The Decazeville kaolinite was treated initially by the De Endredy (1963) method to remove Fe impurities; experiments were performed using the 5 to 10 μm size fraction. Two size fractions (<0.25 and >0.8 μm) were separated from the Glukhovetskoe kaolinite by multiple water column sedimentation. The dickite used in this study was collected from the Baley hydrothermal gold deposit (Russia), where it is found as

* E-mail: schott@lucid.ups-tlse.fr

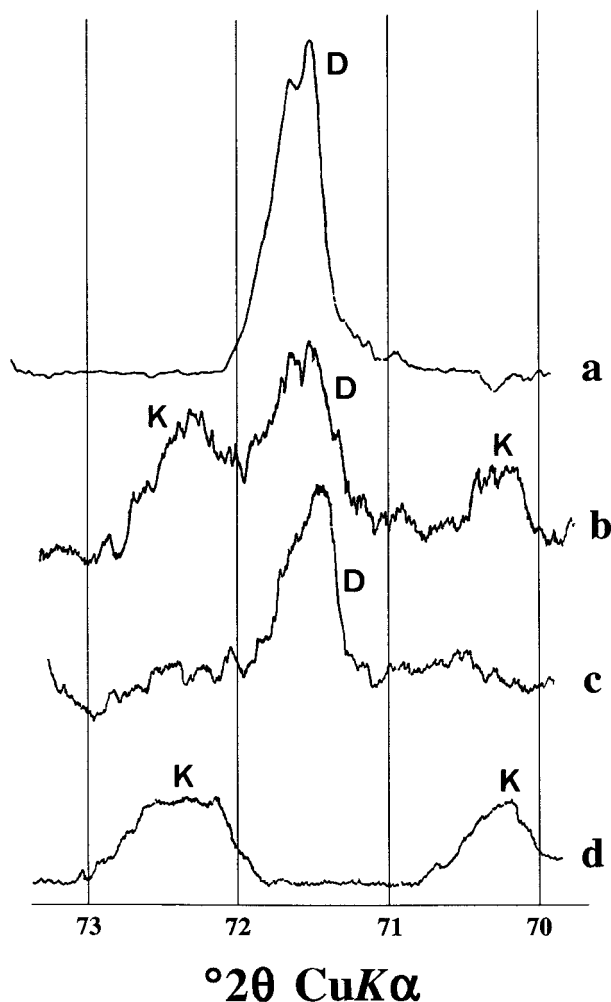


FIGURE 1. Kaolinite and dickite XRD patterns from 70 to 73° 2θ obtained using CuKα radiation (Rusinova et al. 1974). Diagnostic peaks are indicated for kaolinite (K) and dickite (D). Patterns are for (a) dickite-1 (>5 μm), (b) dickite-2 (<3 μm) before experiment, (c) dickite-2 (<3 μm) after experiment, and (d) kaolinite-3.

massive aggregates. Scanning electron microscopy showed that this dickite consists of hexagonal crystals ranging from 2 to 10 μm in diameter and from ~1–2 μm thick. After grinding, the >5 μm and <3 μm size fractions were separated by water column sedimentation (dickite-4 and dickite-5, respectively). X-ray diffraction, performed from 70 to 73° 2θ using CuKα radiation (Rusinova et al. 1974), permits easy distinction between dickite and kaolinite (Fig. 1). All dickite size fractions, except the <3 μm fraction, were kaolinite-free. Only dickite, however, was found in this fraction after reaction at 200 °C for 10–11 days (compare the curves *b* and *c* in Fig. 1). The grain size and specific surface area of the kaolinite and dickite samples used in this study, as measured by Kr and N₂ adsorption using the Brunauer, Emmet, and Teller (BET) method, are listed in Table 1.

TABLE 1. Solid phases used in the present study

Solid phase*	Size fraction (μm)	BET molar surface area (m ² /mol)†	Reference
Glucovetskoe Kaolinite-2	>0.8	1229	Zotov et al. (in preparation)
Gluchovetskoe Kaolinite-3	<0.25	4002	Zotov et al. (in preparation)
Decazeville Kaolinite-4	5–10	654‡	Zotov et al. (in preparation)
Dickite-1	>5	217	This study
Dickite-2	<3	503	This study
Dickite-3	2–10	306‡	This study

* The names of kaolinite samples are the same as in Zotov et al. (in preparation).

† Nitrogen adsorption.

‡ Krypton adsorption.

Experimental design

To avoid possible systematic errors due to uncertainties in the values of aluminum hydrolysis constants and activity coefficients, kaolinite and dickite solubility were measured at the same experimental conditions (temperature, ionic strength, HCl concentration, reactor type, and solution sampling and analysis methods). Experiments were conducted in aqueous HCl at 150 to 300 °C and saturated vapor pressure using various reactor designs. Reactive solutions were prepared by diluting 1N Merck Titrisol standard HCl solution with de-ionized water.

The first set of experiments were performed in ~30 cm³ Teflon-lined titanium autoclaves (alloy BT-8) at temperatures of 150, 200, and 300 °C. These autoclaves were placed in an oven that maintained a constant temperature (to within ±3 °C). The solid/solution mass ratio in the autoclaves was ~2 × 10⁻³. Equilibrium was achieved within about 20, 3, and 1 d at 150, 200, and 300 °C, respectively. The duration of each solubility experiment exceeded the time required to reach equilibrium by at least a factor of 2. At the end of each experiment, the autoclave was quenched and the solution was filtered immediately through a 0.05 μm Millipore filter. About 5 ml of the filtered solution was used for room-temperature pH measurement. Two other subsamples were used for Al and Si analysis. The subsample taken for Si analyses was immediately diluted 10–20 times with de-ionized water to avoid possible precipitation.

A second set of experiments were performed in ~380 cm³ pure titanium autoclaves placed in rocking furnaces to mix the solution and avoid temperature gradients. Experimental temperatures were held constant at 197 and 213 ± 1 °C and measured with an externally calibrated thermocouple [platinum-type S, connected to an RLC (APLTC 3988) reader]. The solid/solution mass ratio was ~6.6 × 10⁻³ at the beginning of the experiment, increasing to ~0.02 at the end as a result of solution sampling. Reactive fluid samples were extracted periodically for pH measurement and Al and Si analysis to monitor the ap-

TABLE 2. Aqueous Al and Si concentrations (at 95% confidence level) in equilibrium with kaolinite and dickite (stoichiometric dissolution) in 0.1 m HCl at 200 °C and in 0.25 m HCl at 300 °C under vapor-saturated conditions

Solid phase	Number of Exper.	Measured Al concentration (10 ⁻³ mol/kg)	Measured Si concentration (10 ⁻³ mol/kg)	Stoichiometric Al and Si concentrations* (10 ⁻³ mol/kg)	Calculated Al ³⁺ concentration (10 ⁻³ mol/kg)	Calculated H ₄ SiO _{4,aq} ⁰ concentration (10 ⁻³ mol/kg)	Calculated pH
200 °C, 0.1 m HCl							
Kaolinite-2 (>0.8 μm)	4	4.77 ± 0.20	5.13 ± 0.36	4.95 ± 0.20	3.52	3.91	1.244
Kaolinite-3 (<0.25 μm)	5	5.38 ± 0.16	5.76 ± 0.20	5.57 ± 0.20	3.86	4.30	1.253
Dickite-4 (>5 μm)	5	4.38 ± 0.06	4.07 ± 0.05	4.22 ± 0.15	3.09	3.43	1.234
Dickite-5 (<3 μm)	5	4.60 ± 0.35	4.38 ± 0.81	4.49 ± 0.20	3.25	3.61	1.238
300 °C, 0.25 m HCl							
Kaolinite-2 (>0.8 μm)	4	7.83 ± 0.64	8.45 ± 0.71	8.14 ± 0.50	4.63	6.34	1.158
Kaolinite-3 (<0.25 μm)	4	8.05 ± 0.39	9.17 ± 1.18	8.61 ± 0.60	4.85	6.64	1.160
Dickite-4 (>5 μm)	5	7.32 ± 0.36	8.14 ± 1.18	7.73 ± 0.35	4.43	6.07	1.155
Dickite-5 (<3 μm)	5	7.46 ± 0.34	8.15 ± 0.15	7.80 ± 0.35	4.47	6.12	1.156

* Average of the measured Al and Si concentrations reported in the previous columns.

proach to equilibrium. The sample used for Si analysis was immediately diluted 10–20 times with H₂O. These fluid samples were initially filtered in situ through a 5 μm titanium filter installed within the autoclave and then filtered a second time at room temperature using a 0.05 μm Millipore filter. After attainment of equilibrium at 197 °C, the temperature was increased to 213 °C and the experiment continued.

Analytical methods

Aqueous aluminum concentrations were determined by flame atomic absorption spectrophotometry (Perkin Elmer Zeeman 5000 and Perkin Elmer 403) and have a 95% confidence limit of ±3%. Silicic acid concentrations were determined colorimetrically (with an uncertainty of ±1.5%) by the molybdate blue method (Koroleff 1976) using a Technicon automated analyzer for the experiments at 150, 197, and 213 °C and a Specord UV-Vis colorimeter for the experiments at 200 and 300 °C.

Thermodynamic calculations

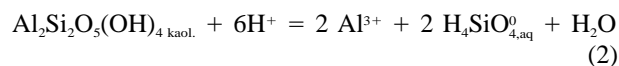
The standard molal Gibbs free energies (ΔG_f^0) and enthalpies (ΔH_f^0) of formation adopted in this study represent the change in those thermodynamic quantities when one mole of a substance in its standard state is formed isothermally from the elements at 1 bar pressure. The standard state for solid phases and H₂O are unit activity for the pure phase at all temperatures and pressures. For aqueous species, the standard state corresponds to unit activity coefficient for a hypothetical ideal one molal solution. Molal activity coefficients of neutral aqueous species were assumed to be unity. Activity coefficients of charged species were calculated using the extended Debye-Hückel equation with values of the electrostatic parameters taken from Helgeson and Kirkham (1974); a value of $\hat{a} = 4.5 \times 10^{-8}$ cm was adopted for all aqueous species.

Taking account of these conventions, the change of Gibbs free energy $\Delta G_{(1)}^0$ for the reaction

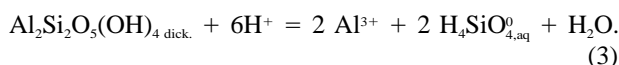


can be generated from kaolinite and dickite solubility measurements performed at the same conditions. In the present study two series of dissolution experiments, involving respectively the stoichiometric and non-stoichiometric dissolution of kaolinite and dickite were performed in aqueous HCl solutions.

Stoichiometric dissolution. At 200 °C with pH < 1.4 and at 300 °C with pH < 0.9, kaolinite and dickite dissolve stoichiometrically (Zotov et al., in preparation). Their dissolution reactions can be expressed as:



and



It follows from the law of mass action of reactions 2 and 3 that for dilute aqueous solutions ($a_{\text{H}_2\text{O}} = 1$) in equilibrium with pure kaolinite and dickite:

$$K_2 = \exp\left(\frac{-\Delta G_{(2)}^0}{RT}\right) = \frac{a_{\text{Al}^{3+}(2)}^2 \cdot a_{\text{H}_4\text{SiO}_{4,\text{aq}}^0(2)}^2}{a_{\text{H}^+(2)}^6} \quad (4)$$

and

$$K_3 = \exp\left(\frac{-\Delta G_{(3)}^0}{RT}\right) = \frac{a_{\text{Al}^{3+}(3)}^2 \cdot a_{\text{H}_4\text{SiO}_{4,\text{aq}}^0(3)}^2}{a_{\text{H}^+(3)}^6} \quad (5)$$

respectively, where K_n denotes the equilibrium constant for the n^{th} chemical reaction, $a_{i(n)}$ designates the equilibrium activity of the i^{th} species in the n^{th} chemical reaction, R is the gas constant, T is absolute temperature, and $\Delta G_{(n)}^0$ represents the Gibbs free energy of the n^{th} reaction. Combining Equations 4 and 5, and the law of mass action for reaction 1 leads to

TABLE 3. $\Delta G_{(1)}^0$ values deduced from stoichiometric kaolinite and dickite solubility measurements reported in Table 2

T (°C)	Reaction	$\Delta \log m_{\text{Al}^{3+}}$ [*] (mol/kg)	$\Delta \log m_{\text{H}_4\text{SiO}_4^0}$ [†] (mol/kg)	ΔpH [‡]	$\Sigma \Delta \S$	$\Delta G_{(1)}^0$ (kcal/mol)
200	Kaolinite 2=Dickite	0.045	0.046	0.008	0.23 ± 0.08	-0.498 ± 0.174
	Kaolinite 3=Dickite	0.086	0.087	0.017	0.448 ± 0.08	-0.970 ± 0.174
300	Kaolinite 2=Dickite	0.017	0.017	0.0025	0.083 ± 0.08	-0.218 ± 0.210
	Kaolinite 3=Dickite	0.037	0.037	0.0045	0.175 ± 0.08	-0.459 ± 0.210

* $\Delta \log m_{\text{Al}^{3+}} = \log m_{\text{Al}^{3+}(2)} - \log m_{\text{Al}^{3+}(3)}$ (see Eqs. 2 and 3).

† $\Delta \log m_{\text{H}_4\text{SiO}_4^0} = \log m_{\text{H}_4\text{SiO}_4^0(\text{aq}(2))} - \log m_{\text{H}_4\text{SiO}_4^0(\text{aq}(3))}$ (see Eqs. 2 and 3).

‡ $\Delta \text{pH} = \text{pH}_{(2)} - \text{pH}_{(3)}$ (see Eqs. 2 and 3).

§ $\Sigma \Delta = 2(\Delta \log m_{\text{Al}^{3+}} + \Delta \log m_{\text{H}_4\text{SiO}_4^0} + 3\Delta \text{pH})$.

|| Average equilibrium concentrations for Dickite-4 and Dickite-5.

$$\begin{aligned}
 \Delta G_{(1)}^0 &= \Delta G_{(3)}^0 - \Delta G_{(2)}^0 \\
 &= 2 \times 2.303RT \{ [\log a_{\text{Al}^{3+}(2)} - \log a_{\text{Al}^{3+}(3)}] \\
 &\quad + [\log a_{\text{H}_4\text{SiO}_4^0(\text{aq}(2))} - \log a_{\text{H}_4\text{SiO}_4^0(\text{aq}(3))}] \\
 &\quad + 3[\text{pH}(2) - \text{pH}(3)] \} \\
 &\cong 2 \times 2.303RT \{ [\log m_{\text{Al}^{3+}(2)} - \log m_{\text{Al}^{3+}(3)}] \\
 &\quad + [\log m_{\text{H}_4\text{SiO}_4^0(\text{aq}(2))} - \log m_{\text{H}_4\text{SiO}_4^0(\text{aq}(3))}] \\
 &\quad + 3[\text{pH}_{(2)} - \text{pH}_{(3)}] \} \quad (6)
 \end{aligned}$$

where $m_{(i)}$ represents the equilibrium molal concentration of the i th aqueous species in the n th reaction.

Non-stoichiometric dissolution. At 200 °C with $\text{pH} > 1.4$ and at 300 °C with $\text{pH} > 0.9$, kaolinite and dickite dissolve incongruently leading to boehmite precipitation according to:



and



for which the law of mass action in dilute aqueous solutions can be expressed as:

$$K_7 = a_{\text{H}_4\text{SiO}_4^0(\text{aq}(7))}^2 \quad (9)$$

and

$$K_8 = a_{\text{H}_4\text{SiO}_4^0(\text{aq}(8))}^2 \quad (10)$$

Combining Equations 9 and 10 with the law of mass action for reaction 1 leads to

$$\begin{aligned}
 \Delta G_{(1)}^0 &= \Delta G_{(8)}^0 - \Delta G_{(7)}^0 \\
 &= 2 \times 2.303RT [\log a_{\text{H}_4\text{SiO}_4^0(\text{aq}(7))} - \log a_{\text{H}_4\text{SiO}_4^0(\text{aq}(8))}] \\
 &\cong 2 \times 2.303RT [\log m_{\text{H}_4\text{SiO}_4^0(\text{aq}(7))} - \log m_{\text{H}_4\text{SiO}_4^0(\text{aq}(8))}] \quad (11)
 \end{aligned}$$

The $\Delta G_{(1)}^0$ from Equations 6 and 11 was calculated using measured total aqueous Al and Si, and quench pH together with aqueous species activities computed with the Gibbs computer code (Shvarov 1992). Distribution of species calculations were generated by assuming the presence of the following aqueous species: H^+ , OH^- , Cl^- ,

HCl^0 , Al^{3+} , AlOH^{2+} , $\text{Al}(\text{OH})_2^+$, $\text{Al}(\text{OH})_3^0$, $\text{AlH}_3\text{SiO}_4^{2+}$, and H_4SiO_4^0 . The stability constants for Al hydroxide complexes were taken from Castet et al. (1993), and those for $\text{AlH}_3\text{SiO}_4^{2+}$ were taken from Pokrovski et al. (1996) and Zotov et al. (in preparation). The dissociation constants for H_2O and H_4SiO_4^0 were taken from SUPCRT92 (Johnson et al. 1992) and that of HCl^0 was taken from Tagirov and Zotov (1995). Thermodynamic parameters for boehmite were taken from Hemingway et al. (1991). Because $\Delta G_{(1)}^0$ values are deduced from kaolinite and dickite solubilities measured at the same temperature and pH conditions and at similar concentrations of aqueous Al, uncertainties associated with calculation of activity coefficients for Al^{3+} impart negligible uncertainties to the computational results.

EXPERIMENTAL RESULTS

Stoichiometric kaolinite and dickite dissolution

The results of kaolinite and dickite solubility measurements performed at 200 and 300 °C are listed in Table 2. For both kaolinite and dickite, equilibrium concentrations of aqueous silica are equal to the corresponding aluminum concentrations, within experimental uncertainty, which demonstrates stoichiometric dissolution. The solubility of the finer grains of kaolinite ($<0.25 \mu\text{m}$) is slightly higher than that of the coarser grains ($>0.8 \mu\text{m}$), especially at 200 °C. Dickite solubility is distinctly lower than that of kaolinite both at 200 and 300 °C. From the analytical data listed in Table 2, the values of pH, and Al^{3+} and H_4SiO_4^0 molalities at equilibrium with kaolinite and dickite were calculated (Table 2) and then used to generate values of the $\Delta G_{(1)}^0$ from Equation 6 (Table 3). These values are negative indicating that dickite is more stable than kaolinite both at 200 and 300 °C.

Non-stoichiometric kaolinite and dickite dissolution

Concentrations of Si and Al measured as a function of time during kaolinite and dickite dissolution experiments performed at 197 and 213 °C are shown in Figure 2. Non-stoichiometric kaolinite and dickite dissolution is characterized by higher Si release relative to Al. In these experiments, Al concentrations reach a maximum prior to attaining steady-state. This non-stoichiometric behavior reflects boehmite precipitation, as confirmed by X-ray diffraction and Raman spectroscopic analyses of the re-

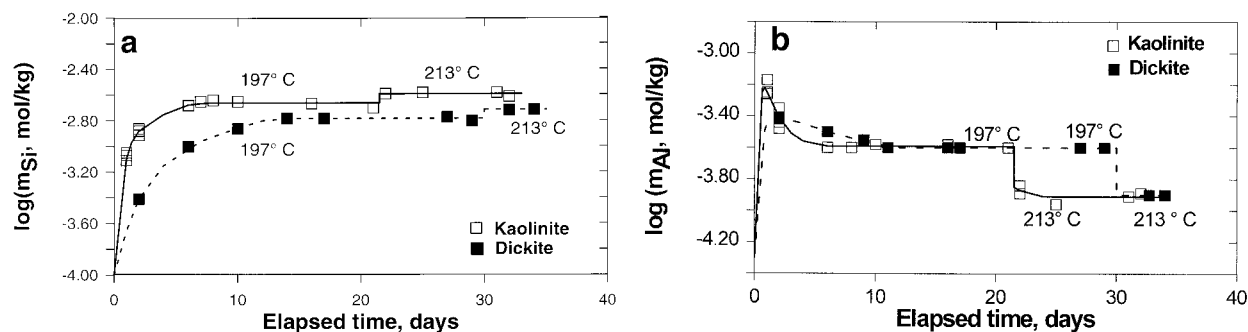


FIGURE 2. The evolution of solution compositions for kaolinite and dickite dissolution experiments at 197 and 213 °C: (a) aqueous Si concentration, (b) aqueous Al concentration.

acted solids. Equilibrium was reached within 20 and 10 d at 150 and 197 °C, respectively. When the experimental temperature was increased from 197, to 213 °C, it took only one day to attain a new steady-state (Fig. 2). Steady-state concentrations of aqueous Si and Al obtained in the experiments performed at 150, 197, and 213 °C are listed in Table 4. Corresponding steady-state concentrations of aqueous Al for kaolinite and dickite solubility are identical, consistent with these concentrations being controlled by boehmite equilibrium. In contrast, steady-state concentrations of aqueous Si are significantly lower for the dickite experiments than for the kaolinite experiments. The values of $\Delta G_{(1)}^0$, deduced from Equation 11 and silica concentrations calculated from measured total Si concentrations are listed in Table 4. Resulting $\Delta G_{(1)}^0$ values are again negative at all temperatures indicating that dickite is more stable than kaolinite.

Effect of kaolinite and dickite surface free energy on solubility

The data listed in Table 2 indicate that dickite solubility is independent of its surface area in the range 200–650

m²/mol. In contrast, the solubility of the <0.25 μm kaolinite size fraction is distinctly higher than that of the coarser size fractions. This solubility increase suggests that the Gibbs free energy of the <0.25 μm kaolinite is 0.4 and 0.24 kcal/mol higher than its coarser-grained counterpart at 200 and 300 °C, respectively. Taking account of the solubility difference between the <0.25 μm and the >0.8 μm kaolinite size fraction and the definition of surface tension (γ_A) given by $\gamma_A = (\delta G/\delta A)_{T,P,n}$, where A designates the mineral surface area and G its Gibbs free energy, yields $\gamma_A = 0.4$ and 0.25 J/m² at 200 and 300 °C, respectively. These γ_A values are slightly higher than those generated from contact angle measurements at 25 °C reported by Janczuk and Bialopiotrowicz (1988) who proposed $\gamma_A = 0.19$ and 0.1 J/m² for a dry and a water-wet (001) face, respectively. Nevertheless, both sets of γ_A values imply that the contribution of the interfacial area to the Gibbs free energy of the >0.8 μm size fractions of kaolinite is negligible [$\delta(\Delta G_{(1)}^0) < 80$ cal/mol]. Assuming a similar value for the surface tension of dickite, it can be assumed that the surface energy of the 2–10 μm dickite size fraction is also insignificant.

TABLE 4. Aqueous Al and Si concentrations (95% confidence level) in equilibrium with the assemblages kaolinite-boehmite and dickite-boehmite (non-stoichiometric dissolution) in 0.03 m HCl at 197 and 213 °C, and in 0.01 m HCl at 150 °C under vapor-saturated conditions and values of $\Delta G_{(1)}^0$

Solid phase	Measured Al concentration (10 ⁻³ mol/kg)	Measured Si concentration (10 ⁻³ mol/kg)	Calculated pH	$\Delta \log m_{\text{H}_4\text{SiO}_4^0, \text{aq}}^*$	$\Delta G_{(1)}^0$ (kcal/mol)
150 °C					
Kaolinite-4 (5–10 μm)	0.19 ± 0.02	0.38 ± 0.03	2.08	-0.16 ± 0.04	-0.620 ± 0.150
Dickite-3 (2–10 μm)	0.20 ± 0.02	0.26 ± 0.02	2.08		
197 °C					
Kaolinite-4 (5–10 μm)	0.26 ± 0.01	2.19 ± 0.15	1.65	-0.12 ± 0.03	-0.516 ± 0.130
Dickite-3 (2–10 μm)	0.25 ± 0.01	1.66 ± 0.04	1.65		
213 °C					
Kaolinite-4 (5–10 μm)	0.12 ± 0.01	2.57 ± 0.12	1.65	-0.12 ± 0.02	-0.534 ± 0.090
Dickite-3 (2–10 μm)	0.13 ± 0.01	1.95 ± 0.04	1.65		

* $\Delta \log m_{\text{H}_4\text{SiO}_4^0, \text{aq}} = \log m_{\text{H}_4\text{SiO}_4^0, \text{aq}(7)} - \log m_{\text{H}_4\text{SiO}_4^0, \text{aq}(8)}$ (see Eqs. 7 and 8).

Thermodynamic parameters of the kaolinite ↔ dickite reaction

Values of $\Delta G_{(1)}^0$ were generated from dickite and >0.8 μm kaolinite solubilities determined at the same temperature and pH conditions (Table 5). Values of $\Delta G_{(1)}^0$ at 25 °C and 1 bar were derived from $\Delta G_{(1)}^0$ values determined in this study together with standard entropy (S^0), heat capacity (C_p^0) and volume (V^0) data for kaolinite and dickite taken from the literature. The C_p^0 and S^0 values of dickite and kaolinite reported by Haas et al. (1981) were used to derive the ΔC_p^0 and ΔS^0 for reaction 1:

$$\Delta C_{p(1)}^0 = 38.05 - 18.14 \times 10^{-3}/T + 5.53 \times 10^5/T^2 - 69.71 \times 10/T^{0.5} \quad (12)$$

$$\Delta C_{p(1),298}^0 = -1.52 \text{ cal/mol}\cdot\text{K} \quad (13)$$

$$\Delta S_{(1),298}^0 = -1.90 \text{ cal/mol}\cdot\text{K}. \quad (14)$$

Although a different value of S^0 for kaolinite was proposed by Robie and Hemingway (1991), those of Haas et al. (1981) were adopted in the present study because they originated from the calorimetric measurements performed on both minerals by King and Weller (1961). The volume for reaction 1 ($\Delta V_{(1)}^0$) was calculated using data generated by Ehrenberg et al. (1993), which are based on the structural determinations of Bish and Von Dreele (1989) and Joswig and Drits (1986). The resulting $\Delta V_{(1)}^0$ value is $-0.77 \text{ cm}^3/\text{mol}$, which implies only a small variation of $\Delta G_{(1)}^0$ with pressure. For example, $\Delta G_{(1)}^0$ decreases by only 20 cal/mol if pressure increases from 1 to 1000 bars. Consequently, the effect of pressure on the kaolinite ↔ dickite equilibrium is negligible.

Taking account of the above parameters and the equation

$$\Delta G_{(1),T}^0 = \Delta G_{(1),298}^0 - \Delta S_{298}^0(T - 298) + \int_{298}^T \Delta C_p^0 dT + \int_{298}^T \Delta C_p^0 d \ln T \quad (15)$$

enables determination of the standard Gibbs free energy of reaction 1 at 298 K [$\Delta G_{(1),298}^0$] from the high-temperature data reported in Tables 3 and 4. The results of this analysis reported in Table 5 yield $\Delta G_{(1),298}^0 = -0.90 \pm 0.10 \text{ kcal/mol}$. Moreover, these $\Delta G_{(1),298}^0$ data were used together with Equations 12–15 to compute $\Delta G_{(1)}^0$ as a function of temperature. The results of this calculation are illustrated in Figure 3 where it can be seen that $\Delta G_{(1)}^0$ is negative, indicating that kaolinite is metastable relative to dickite at temperatures from 25 to at least 300 °C, which are conditions typical of weathering, sedimentary, and hydrothermal processes. According to these calculations, equilibrium between kaolinite and dickite is attained at ~ 425 °C. Note, however, that above 300 °C neither kaolinite nor dickite are stable with respect to pyrophyllite and andalusite in quartz saturated aqueous solutions (Hemley et al. 1980).

The standard Gibbs free energy of formation of dickite ($\Delta G_{f,298}^0$) was generated from the $\Delta G_{(1),298}^0$ value determined in this study and from the $\Delta G_{f,298}^0$ of kaolinite derived by Zotov et al. (in preparation), using solubility measurements reported in this study. It should be noted that the value of the Gibbs free energy of formation of kaolinite determined by Zotov et al. ($\Delta G_{f,298}^0 = -907.46 \text{ kcal/mol}$) is very close to that proposed by Devidal et al. (1996) ($\Delta G_{f,298}^0 = -907.68 \text{ kcal/mol}$). Additional consistent thermodynamic properties for dickite are available in the literature. The S_{298}^0 of dickite can be calculated from S_{298}^0 of kaolinite (Robie and Hemingway 1991) and $\Delta S_{(1),298}^0$ determined by King and Weller (Haas et al. 1981). The coefficients for the heat capacity equation and the value of V_{298}^0 are given by Haas et al. (1981) and Ehrenberg et al. (1993), respectively. Thermodynamic parameters for dickite generated in this study and for kaolinite reported by Zotov et al. (in preparation) are listed in Table 6.

DISCUSSION

Consistency between the results of this study and petrographic observations of the kaolinite to dickite transformation

In contrast to the thermodynamic parameters for kaolinite and dickite reported by Naumov et al. (1974), Robie et al. (1979), Haas et al. (1981), and Robinson et al. (1982), the data generated in this study indicate that dickite is the stable polytype of the kaolin group of clay minerals to at least 350 °C. According to results obtained in the present study, the massive kaolinite to dickite transformation documented in many natural systems is an irreversible process, controlled by the kinetics rather than the thermodynamics of these minerals. Therefore, it seems likely that the formation and preservation of kaolinite over long time periods in surficial environments are controlled by the relative dissolution and precipitation rates of these two polytypes.

It has been long recognized that kaolinite to dickite transformation occurs in sedimentary basin sandstones with increasing burial depth and temperature (Smithson 1954; Kossovskaya and Shutov 1963; Shutov et al. 1970; Ehrenberg et al. 1993). According to Kossovskaya and Shutov (1963), the extent of this transformation is time-dependent. These authors observed a kaolinite to dickite transformation at a depth of 2.5 km in Mesozoic layers of the Siberian platform but at a depth of 1.0–1.5 km in older Riphean and early Paleozoic deposits of the Russian platform. Ehrenberg et al. (1993) recently studied the kaolinite to dickite transformation as a function of burial depth in three different Norwegian continental shelf basins where dickite replaces kaolinite at ~ 3.1 – 3.4 km below the sea floor (120–130 °C). Also, Ehrenberg et al. (1993) observed consistent differences in crystal morphology between the kaolinite-dominated and dickite-dominated samples, implying that the kaolinite to dickite transformation occurs by a dissolution-reprecipitation mechanism.

TABLE 5. Values of $\Delta G_{(1)}^0$ for the reaction kaolinite \leftrightarrow dickite

T ($^{\circ}\text{C}$)	$\Delta G_{(1),\text{exp}}^0$ (kcal/mol)	$\Delta G_{(1),298.15, 1 \text{ bar}}^0$ (kcal/mol)*
150	$-0.62(0) \pm 0.150$	-0.88 ± 0.15
197	-0.516 ± 0.130	-0.89 ± 0.13
200	-0.498 ± 0.174	-0.88 ± 0.17
213	-0.534 ± 0.090	-0.94 ± 0.09
300	-0.218 ± 0.210	-0.82 ± 0.21
Average $\Delta G_{(1),298.15, 1 \text{ bar}}^0 = -0.90 \pm 0.10$		

* $\Delta G_{(1),298.15, 1 \text{ bar}}^0$ was derived from $\Delta G_{(1),\text{exp}}^0$ at a given T using Equation 12 together with $\Delta S_{(1),298}^0 = -1.90 \text{ cal/mol}\cdot\text{K}$.

Dickite also forms in hydrothermally altered rocks and veins in the temperature range 150–270 $^{\circ}\text{C}$. Observations of active hydrothermal systems confirm that dickite generally does not form in low-temperature solfataric fields (<100–120 $^{\circ}\text{C}$) where kaolinite is ubiquitous. In contrast, dickite forms at higher temperature (150–270 $^{\circ}\text{C}$) in deeper, altered zones (Hayashi 1973; Andreeva and Zotov 1982). It is likely that at these temperatures, dickite precipitates directly from supersaturated solutions without the transient formation of kaolinite.

If dickite is the stable kaolin polytype, the pervasive presence of kaolinite in subsurface environments probably reflects lower rates and higher activation energies for the nucleation and crystal growth of dickite than for kaolinite. An increase in temperature to about 120–150 $^{\circ}\text{C}$ is required for the nucleation and precipitation rates of dickite to match those of kaolinite. Accordingly, the transformation of metastable kaolinite to stable dickite with increasing depth of burial in sedimentary basins appears to be kinetically controlled. As a result, unlike the suggestion of Ehrenberg et al. (1993), the kaolinite-dickite reaction cannot be used as a reliable paleogeothermometer. For such an application, reliable nucleation and crystal growth kinetic data are required for both kaolinite and dickite.

Halloysite, a kaolinite polymorph, provides another example of metastability in the system $\text{Al}_2\text{Si}_2\text{O}_5(\text{OH})_4$. Although it is undoubtedly less stable than kaolinite [the standard Gibbs free energy of the halloysite \leftrightarrow kaolinite reaction is about -4 kcal/mol according to Robie et al. (1979), Robinson et al. (1982), and Anovitz et al. (1991)], halloysite commonly forms at low temperatures in both nature and experiments from solutions supersaturated with respect to these two polymorphs. However, the activation energy barrier for the halloysite to kaolinite transformation is markedly lower than that for the reaction of kaolinite to dickite because the former transformation occurs in both surficial environments and experiments carried out at $T < 50 \text{ }^{\circ}\text{C}$ (La Iglesia and Galan 1975; Tsuzuki and Kawabe 1983).

Thermodynamic properties of 1:1 and 2:1 layers aluminosilicate polytypes

The thermodynamic properties of the kaolinite-dickite polytypic transformation can be compared to those of the equivalent muscovite reactions. The most commonly oc-

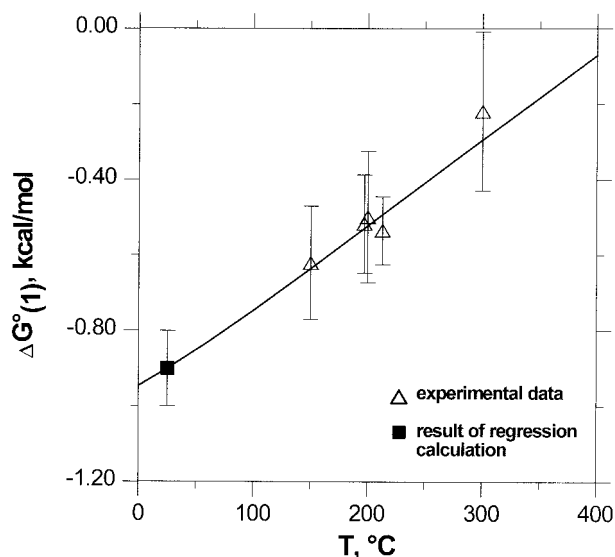


FIGURE 3. Gibbs free energy $\Delta G_{(1)}^0$ of the reaction Kaolinite \leftrightarrow Dickite as a function of temperature. The solid line shows the fit of experimental results at temperatures 150, 197, 200, 213, and 300 $^{\circ}\text{C}$ using the data from Haas et al. (1981) for S_{298}^0 and $C_p^0 = f(T)$, and from Ehrenberg et al. (1993) for V_{298}^0 . Triangles = experimental data, filled box = fitted value of $\Delta G_{(1)}^0$ at 25 $^{\circ}\text{C}$ and 1 bar.

curing muscovite polymorphs are 1M (analogous to kaolinite) and $2M_1$ (analogous to dickite). Several experimental studies have focused on the reaction muscovite 1M \leftrightarrow muscovite $2M_1$ at temperatures to 700 $^{\circ}\text{C}$ and pressures to 7 kb (Yoder and Eugster 1955; Velde 1965; Mukhamet-Galeev et al. 1985, 1992). Similar to what was found in the present study for the kaolin group of clay minerals, the double layer $2M_1$ is the only stable muscovite polytype. The standard Gibbs free energy of the 1M to $2M_1$ reaction at 25 $^{\circ}\text{C}$ ($\Delta G^0 = -1.7 \pm 0.6 \text{ kcal/mol}$, Mukhamet-Galeev et al. 1985) is close to that determined in this study for the equivalent kaolinite group reaction. The apparent activation energy for this transformation as determined by Mukhamet-Galeev et al. (1985) using the approach taken by Wood and Walther (1983), however, is high ($E_A = 51 \pm 10 \text{ kcal/mol}$). This high E_A value is consistent with the geological observations of Loginov et al. (1976a, 1976b) which show that the 1M to $2M_1$ transformation occurs in the temperature range 300–350 $^{\circ}\text{C}$ (greenschist facies). Considering the 120–150 $^{\circ}\text{C}$ temperature observed for the dickite-kaolinite replacement reaction in sedimentary basins, it seems likely that the apparent activation energy for this transformation is lower than that for muscovite.

Although the double-layer polytypes are the stable phases of the kaolinite and muscovite groups, they do not form directly from low-temperature solutions. Mono-layer polytypes formed in low-temperature environments transform into double-layer polytypes with increasing temperature and pressure as shown by numerous geological (Velde 1965; Kossovskaya and Drits 1971; Omel-

TABLE 6. Thermodynamic data at 25° C and 1 bar and heat capacity power function coefficients for dickite and kaolinite

Mineral	$\Delta G_{f,298}^{\circ}$ (kcal/mol)	$\Delta H_{f,298}^{\circ}$ (kcal/mol)	S_{298}° (cal/mol-K)	$C_{p,298}^{\circ}$ (cal/mol-K)	V_{298}° (cm ³ /mol)	<i>a</i>	<i>b</i>	<i>c</i>	<i>d</i>
Dickite	-908.355* ±0.400	-985.736* ±0.600	46.116* ±1.0	57.310†	98.58‡	217.1032†	-50.50822†	9.09285†	-267.5743†
Kaolinite	-907.455§ ±0.300	-984.270§ ±0.500	48.016 ±0.12	58.828†	99.35‡	179.0571†	-32.36625†	3.56585†	-197.8642†

Heat capacity equation: C_p° (cal/mol-K) = $a + b \times 10^{-3} \cdot T + c \times 10^5/T^2 + d \times 10/T^3$

* This study.

† Haas et al. (1981).

‡ Ehrenberg et al. (1993).

§ Zotov et al. (in preparation).

|| Hemingway et al. (1991).

yanenko et al. 1982) and experimental (Yoder and Eugster 1955; Velde 1965; Mukhamet-Galeev et al. 1985, 1992) observations. The morphological difference in co-existing 1:1 and 2:1 layer polytypes suggest that this transformation occurs by dissolution and precipitation rather than by solid-state diffusion.

Thermodynamic data for transformations among polytypes of kaolin group are similar to those for the muscovite polytypes. This confirms that the double-layer kaolinite and muscovite polytypes, which exhibit a lesser degree of disorder, are also more stable than the one-layer polytypes. However, in solutions supersaturated with respect to both polytypes, nucleation and crystal growth of the more-disordered 1M phase is easier than that of the 2M₁ phases with limited degree of disorder. This is illustrated by high values of the apparent activation energy measured by Mukhamet-Galeev et al. (1985) for the 1M-2M₁ transformation in muscovite.

ACKNOWLEDGMENTS

We thank J.-L. Devidal for supplying Decazeville kaolinite and Z.Y. Kotova, G.E. Kalenchuk, J. Escalier, and J.-M. Gautier for assistance in chemical analyses. We also thank J.-M. Gautier for surface area measurements using the B.E.T. method. We are very grateful to J.-L. Dandurand, J.-L. Devidal, E. Oelkers, and G. Pokrovski for helpful discussions during the course of this study. We are very grateful to E. Oelkers for his comments and corrections of the manuscript. Constructive reviews by H. May, D. Wesolowski, and an anonymous reviewer led to significant improvements to the text. Special thanks are due to Y. Shvarov for providing his computer program GIBBS. Support from the French Ministère de l'Enseignement Supérieur et de la Recherche (awarding of a triennial visiting professorship to A.Z.) and the Institut Français du Pétrole is gratefully acknowledged.

REFERENCES CITED

- Andreeva, O.V. and Zotov, A.V. (1982) Metasomatic zoning in altered rocks in active geothermal areas. In N.N. Pertsev, Ed., *Problems of Vertical Metasomatic Zoning*, p. 14–36. Nauka, Moscow (in Russian).
- Anovitz, L.M., Perkins, D., and Essene, E.J. (1991) Metastability in near-surface rocks of minerals in the system Al₂O₃-SiO₂-H₂O. *Clays and Clay Minerals*, 39, 225–233.
- Bailey, S.W. (1980) Structures of layer silicates. In G.W. Brindley and G. Brown, Eds., *Crystal Structures of Clay Minerals and their X-ray Identification*, p. 1–123. Mineralogical Society, London.
- Bish, D.L. and Von Dreele, R. (1989) Reitveld refinement of non-hydrogen atomic position in kaolinite. *Clays and Clay Minerals*, 37, 289–296.
- Castet, S., Dandurand, J.-L., Schott, J., and Gout, R. (1993) Boehmite solubility and aqueous aluminum speciation in hydrothermal solutions (90–350 °C): Experimental study and modelling. *Geochimica et Cosmochimica Acta*, 57, 4869–4884.
- De Endrey, A.S. (1963) Estimation of free iron oxides in soils and clays by a photolytic method. *Clay Minerals Bulletin*, 5, 209–217.
- Devidal, J.-L., Dandurand, J.-L., and Gout, R. (1996) Gibbs free energy of kaolinite from solubility measurement in basic solution between 60 and 170 °C. *Geochimica et Cosmochimica Acta*, 60, 553–564.
- Dunoyer de Segonzac, G. (1970) Clay-minerals diagenesis and low-grade metamorphism. *Sedimentology*, 15, 281–346.
- Ehrenberg, S.N., Aagaard, P., Wilson, M.J., Fraser, A.R., and Duthie, D.M.L. (1993) Depth-dependent transformation of kaolinite to dickite in sandstones of the Norwegian continental shelf. *Clay Minerals*, 28, 325–352.
- Haas, J.L., Jr., Robinson, G.R., Jr., and Hemingway, B.S. (1981) Thermodynamic tabulations for selected phases in the system CaO-Al₂O₃-SiO₂-H₂O at 101.325 kPa (1 atm) between 273.15 and 1800 K. *Journal of Physical and Chemical Reference Data*, 10, 575–669.
- Hayashi, M. (1973) Hydrothermal alteration in the Otake geothermal area, Kyushu. *Journal of Japanese Geothermal Energy Association*, 10, 9–46.
- Hemley, J.J., Montoya, J.W., Marinenko, J.W., and Luce, R.W. (1980) Equilibria in the system Al₂O₃-SiO₂-H₂O and some general implications for alteration/mineralization processes. *Economic Geology*, 75, 210–228.
- Hemingway, B.S., Robie, R.A., and Apps, J.A. (1991) Revised values for the thermodynamic properties of boehmite, AlO(OH), and related species and phases in the system Al-O-H. *American Mineralogist*, 76, 445–457.
- Janczuk, B. and Bialopiotrowicz, T. (1988) Components of surface free energy of some clay minerals. *Clays and Clay Minerals*, 36, 243–248.
- Johnson, J.W., Oelkers, E.H., and Helgeson, H.C. (1992) SUPCRT92. A software package for calculating the standard molal thermodynamic properties of minerals, gases, aqueous species, and reactions from 1 to 5000 bar and 0 to 1000 °C. *Computer and Geosciences*, 18, 899–947.
- Joswig, W. and Drits, V.A. (1986) The orientation of the hydroxyl groups in dickite by X-ray diffraction. *Neues Jahrbuch für Mineralogie Monatshefte*, 1, 19–22.
- King, E.G. and Weller, W.W. (1961) Low-temperature heat capacities and entropies at 298.15° K of diaspore, kaolinite, dickite, and halloysite. United States Bureau of Mines Report Investigation 5810.
- Koroleff, F. (1976) Determination of silicon. In K. Grasshoff, Ed., *Methods of Seawater Analysis*, p. 149–158. Springer-Verlag, Berlin.
- Kossovskaya, A.G. and Shutov, V.D. (1963) Facies of regional epi- and metagenesis. *International Geology Review*, 7, 1157–1167.
- Kossovskaya, A.G. and Drits, V.A. (1971) Problems bearing on crystal and genetic classification of micaceous minerals from sedimentary rocks. In *Epigenesis and its Mineral Indicators*, p. 71–95. Trudy Geologicheskogo Instituta AN SSSR, 221, Nauka, Moscow (in Russian).
- La Iglesia, A. and Galan, E. (1975) Halloysite-kaolinite transformation at room temperature. *Clays and Clay Minerals*, 23, 109–113.
- Loginov, V.P., Pirozhok, P.I., and Rusinov, V.L. (1976a) Wall rock alteration zoning at the Uchaly massive sulphide deposits (South Urals). *Geokhimiya, Mineralogiya, Petrologiya Sofia*, 5, 93–101 (in Russian).

- Loginov, V.P., Arakeljanc, M.M., Gradusov, B.P., Lomeyko, E.I., Mkhitar-yan, R.K., and Piloyan, G.O. (1976b) Geological age of Levikha massive sulphide deposits and K-Ar age variations of wall rock sericites. *Doklady Akademii Nauk SSSR*, 231, 937–940 (in Russian).
- Mukhamet-Galeev, A.P., Pokrovskii, V.A., Zotov, A.V., Ivanov, I.P., and Samotoin, N.D. (1985) Kinetics and crystallization of hydrothermal muscovite 2M₁ (experimental study). *Izvestia Akademii Nauk USSR, Seria Geologicheskaya*, N 10, 63–75 (in Russian).
- Mukhamet-Galeev, A.P., Zotov, A.V., and Kotova, Z.Y. (1992) Thermodynamic properties of 2M₁ and 1M muscovite polytypes. *Geokhimiya*, N 2, 238–248 (in Russian).
- Naumov, G.B., Ryzhenko, B.N., and Khodakovskiy, I.L. (1974) *Handbook of Thermodynamic Data*. U.S. Geological Survey, Report PB226–722, 328 p.
- Omelyanenko, B.I., Volovikova, I.M., and Drits, V.A. (1982) On the notion sericite. *Izvestia Akademii Nauk USSR, Seria Geologicheskaya*, N 5, 69–87 (in Russian).
- Pokrovskii, G.S., Schott, J., Harrichoury, J.-C., and Sergeyev, A.S. (1996) The stability of aluminum silicate complexes in acidic solutions from 25 to 150 °C. *Geochimica et Cosmochimica Acta*, 60, 2495–2501.
- Robie, R.A., Hemingway, B.S., and Fisher, J.R. (1979) Thermodynamic properties of minerals and related substances at 298.15 K and 1 bar (10⁵ pascals) pressure and at higher temperatures. *Geological Survey Bulletin* 1452.
- Robie, R.A. and Hemingway, B.S. (1991) Heat capacities of kaolinite from 7 to 380 K and of DMSO-intercalated kaolinite from 20 to 310 K. The entropy of kaolinite Al₂Si₂O₅(OH)₄. *Clays and Clay Minerals*, 39, 362–368.
- Robinson, G.R., Haas, J.L., Jr., Schafer, C.M., and Haselton, H.T. (1982) Thermodynamic and thermophysical properties of selected phase in the MgO-SiO₂-H₂O-CO₂, CaO-Al₂O₃-SiO₂-H₂O-CO₂, and Fe-FeO-Fe₂O₃-SiO₂ chemical systems, with special emphasis on the properties of basalts and their mineral components. United States Geological Survey Open-File Report 83–79.
- Rusinova, O.V., Piloyan, G.O., Rusinov, V.L., Samotoin, N.D., and Fedotov, A.F. (1974) Diagnostics of nacrite. In *Trudy Central Institute of Geological Research USSR (CNIGRI)*, 112, 11–28 (in Russian).
- Shutov, V.D., Aleksandrova, A.V., and Losievskaya, S.A. (1970) Genetic interpretation of the polymorphism of the kaolinite group in sedimentary rocks. *Sedimentology* 15, 69–82.
- Shvarov, Y.V. (1992) The software for equilibrium modeling of hydro-chemical processes. Abstract of the 2nd International Symposium Thermodynamics of Natural Processes (TNP-2), Novosibirsk, 1992.
- Smithson, F. (1954) The petrography of dickite sandstones in North Wales and northern England. *Geological Magazine*, 91, 177–188.
- Tagirov, B.R. and Zotov, A.V. (1995) An experimental study of hydrochloric acid ionization at 400–500° C and 500–2500 bars: Thermodynamic properties of HCl_{aq} at temperatures of 25–700°C and pressures to 4 kbars. In Y.K. Kharaka and O.V. Chudayev, Eds., *Water-Rock Interaction (WRI-8)*, p. 837–840. A.A. Balkema, Rotterdam.
- Tsuzuki, Y. and Kawabe, I. (1983) Polymorphic transformations of kaolin minerals in aqueous solutions. *Geochimica et Cosmochimica Acta*, 47, 59–66.
- Velde, B. (1965) Experimental determination of muscovite polymorph stabilities. *American Mineralogist*, 50, 436–449.
- Wood, B.J. and Walther, J.V. (1983) Rates of hydrothermal reactions. *Science*, 222, 413–415.
- Yoder, H.S. and Eugster, H.P. (1955) Synthetic and natural muscovites. *Geochimica et Cosmochimica Acta*, 8, 255–280.

MANUSCRIPT RECEIVED JULY 16, 1997

MANUSCRIPT ACCEPTED DECEMBER 4, 1997

PAPER HANDLED BY J. WILLIAM CAREY